Non-linear Model Fitting to Parameterize Diseased Blood Vessels

Alexandra La Cruz*
Vienna University of Technology
Miloš Šrámek§
Austrian Academy of Sciences
Matúš Straka†
Austrian Academy of Sciences
Eduard Gröller¶
Vienna University of Technology
Arnold Köchl‡
Vienna University of Medicine
Dominik Fleischmann‖
Stanford University Medical Center

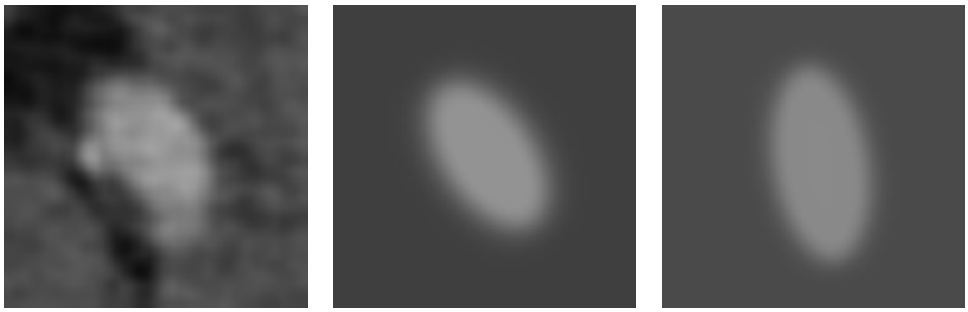

(a) (b) (c)

Figure 1: Cross-section view of a vessel (a) and the best fitted model (b) from an initial model (c)

ABSTRACT

Accurate estimation of vessel parameters is a prerequisite for automated visualization and analysis of normal and diseased blood vessels. The objective of this research is to estimate the dimensions of lower extremity arteries, imaged by computed tomography (CT). The vessel is modeled using an elliptical or cylindrical structure with specific dimensions, orientation and blood vessel mean density. The model separates two homogeneous regions: Its inner side represents a region of density for vessels, and its outer side a region for background. Taking into account the point spread function (PSF) of a CT scanner, a function is modeled with a Gaussian kernel, in order to smooth the vessel boundary in the model. A new strategy for vessel parameter estimation is presented. It stems from vessel model and model parameter optimization by a nonlinear optimization procedure (the Levenberg-Marquardt technique). The method provides center location, diameter and orientation of the vessel as well as blood and background mean density values. The method is tested on synthetic data and real patient data with encouraging results.

CR Categories: I.4.3 [Image Processing and Computer Vision]: Enhancement—Geometric Correction; I.4.6 [Segmentation]: Edge and Feature Detection—; I.5.1 [Pattern Recognition]: Models—Geometric;

Keywords: Visualization, Segmentation, Blood Vessel Detection

1 INTRODUCTION

Peripheral arterial occlusive disease (PAOD) is a manifestation of atherosclerosis. It is characterized by the formation of atherosclerotic plaque on the inner surface of the vessel wall, which protrudes into the vessel lumen, causing luminal narrowing (stenosis) or complete vessel occlusion. The reduced blood flow to the legs at first causes cramping with exercise or walking, and, at later stages of the disease, rest pain, and tissue loss, which may eventually require amputation. Vascular imaging plays a pivotal role for diagnosis, staging, and treatment planning in patients with PAOD. Computed tomography angiography (CTA) has recently evolved into a routinely applicable imaging technique to visualize the entire peripheral (lower extremity) arterial tree. A peripheral CTA dataset consists of up to 2000 transverse CT slices, and thus cannot be assessed by the radiologist or treating physician without further image post-processing. Accurate and automated extraction of the peripheral arterial tree from peripheral CTA datasets is thus highly desirable.

This is not a trivial task, however, particularly in the presence of atherosclerotic disease. Normal arteries are characterized by a fairly homogenous CT density of the vessel lumen due to the contrast-medium enhanced blood, which is higher in x-ray attenuation than the surrounding soft tissues (muscles, fat), and which is generally lower in attenuation than neighbouring bony tissue. Diseased arterial segments, however, may have very different x-ray attenuation. Non-calcified atherosclerotic plaque is isodense to soft tissues, and calcified plaque has a CT density similar to bone. Hence, it is not surprising that density and gradient information alone is insufficient to accurately extract the centerlines of a diseased arterial tree. This overlap in density ranges is further aggravated by the wide range of diameters observed for individual branches of the arterial tree, as well as by the presence of image noise, scanning artifacts, limited scanner resolution with partial volume averaging, and finally, inter-individual and within-patient variability of arterial opacification.

The most characteristic feature of an artery (normal or diseased) is its cylindrical or tubular shape. A tubular or cylindric shape can be modeled as elliptical or circular cross-sections along its medial axis, and then fitted to a candidate vascular structure. As a result of the estimated vessel diameter and density, a more robust extraction of a vessel centerline, even in the presence of atherosclerotic disease, is expected. We are particularly interested in finding a model that best fits the data satisfying both criteria, tubular shape

*alacruz@cg.tuwien.ac.at
†matus.straka@oeaw.ac.at
‡arnold.koechl@univie.ac.at
§milos.sramek@oeaw.ac.at
¶groeller@cg.tuwien.ac.at
‖d.fleischmann@stanford.edu

and mean density value.

In this work, we propose two new strategies to estimate vessel parameters from an initial vessel model using a non-linear minimization process. The first strategy attempts to fit an elliptical cross-section-model to the vessel. The second strategy uses a 3D cylindrical model of the vessel.

The paper is divided into six sections. Section 2 provides an overview of related approaches concerning model based segmentation techniques applied to vascular structure. Section 3 describes the main motivation of this work and the importance of extracting a better parameterization of diseased blood vessels. Section 4 presents the non-linear model fitting technique using an elliptical cross-section (in 2D) and cylindrical shape (in 3D). In section 5 we present and discuss our results and finally, in section 6 draw the conclusions of this work.

2 Related Work

Kirbas et al. [3] classified several segmentation methods according to the technique used. They demonstrated that there is no single segmentation method that allows to extract the vasculature across different medical imaging and not even for different vascular anatomic territories. Some methods use threshold values, or an explicit vessel model to extract contours. Other techniques require image processing (depending on the data, quality, noise, artifacts), a priori segmentation or post-processing.

Deformable models [7] and multiscale methods [4] have been used more recently, and appear to be the most promising segmentation techniques. Deformable models are powerful and widely used methods for segmentation and geometric model generation in 2D and 3D data [1]. They can be used in any modality [3]. These techniques are based on a minimization process of an energy function. This energy function involves internal and external forces. The internal forces allow smoothness on the contour and the external forces move the deformable structure towards edges. Depending on the definition of the energy function, it can inflate or shrink towards the object. Nevertheless, these techniques are strongly dependent on the initialization. The energy function uses the gradient information or derivative values around the deformable object. In constrasct, multiscale methods [4] are based on the extraction of large structures at low resolution images and fine structures at high resolution. Multiscale filtering uses the Hessian matrix which contains the second derivatives of the data. Our experimental results on synthetic and real clinical data suggest, however, [5] that even the gradient information and derivatives are not sufficient to accurately extract the centerlines of peripheral arteries. This is due to the overlapping of density values between vascular and non-vascular structures, the variability in opacification between patients and from aorta to pedal vessels, image noise, and partial volume averaging.

Classical model based segmentation algorithms [1, 3] applied to vessel extraction are based on fitting circular, elliptical or cylindrical geometric models to the data. Such techniques combine thresholds with gradient information [12] or derivative estimation [4] in order to approximate the vessel boundary. Then, this initial boundary estimation is fitted to a geometrical model (circular or elliptical cross-section or cylindrical structure).

3 Motivation for a Model-Based Vessel Parameterization

Automatic segmentation and accurate centerline identification of diseased arteries certainly is a challenge. We are currently using a density and gradient based vessel tracking and centering technique to process clinical cases of patients with PAOD [2]. In patients with extensive disease, however, substantial expert user interaction and manual corrections are necessary to bridge the segments where standard segmentation fails. Figure 2 is an illustration of extensively diseased vessel territories where expert user interaction was required to generate images of adequate diagnostic quality. In this case, a technique capable of identifying the vessel by its cylindrical or tubular shape might have yielded a similar or better result in determining the center-line. This would improve the visualization technique actually used in the clinical environment, which is mostly Curved Planar Reformation (CPR) and its extensions [2].

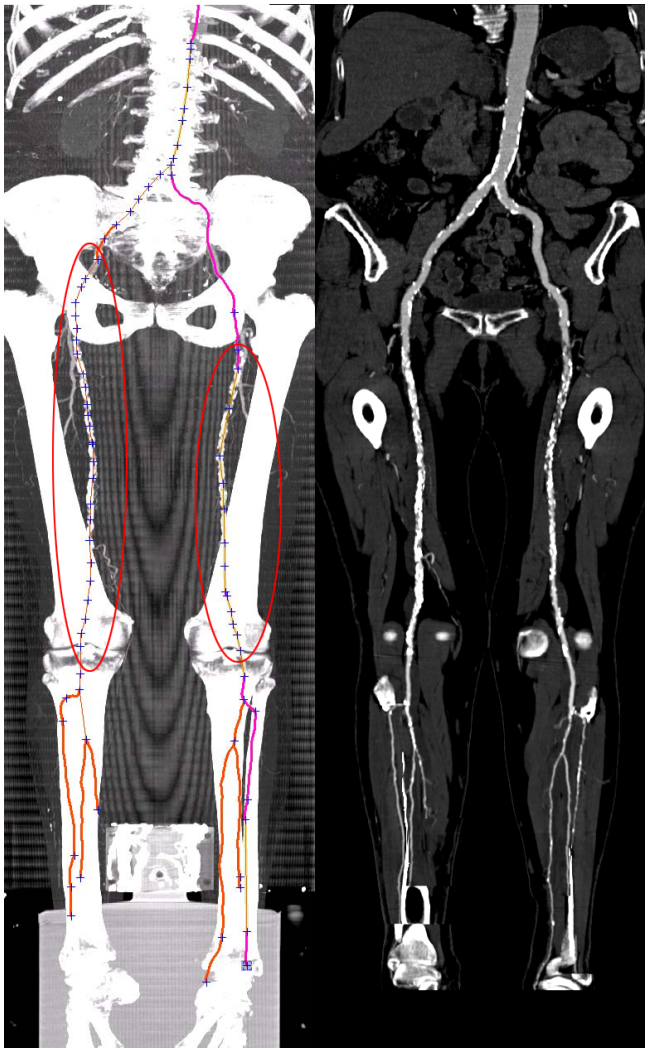

Figure 2: MIP image (left) of a clinical peripheral CTA dataset obtained in a patient with advanced peripheral arterial disease with superimposed tree of vessel-centerlines. The encircled areas indicate vessel regions, where automated centerline calculations failed due to excessive disease and vessel calcifications, and thus required manual placement of center points by a radiologist, to achieve the resulting Curved Planar Reformation (right).

4 Non-Linear Model Fitting

In this paper, we present two different vessel models. An elliptical model in 2D and a cylindrical model in 3D. Each model has a set of unknown parameters, which are estimated by minimization of a χ^2-based merit function. Both methods require an initial estimation of the parameters. They can either be obtained from the centerline

defined by vessel tracking, or the previous slices, which requires only an initial seed point.

We represent the vessel by a 2D (ellipse in a slice) or 3D (cylinder) implicit model f. The CT-Scanner, due to finite dimensions of its detectors, blurs the data, which leads to partial volume effects (PVE) [10]. This can be modeled by a nonideal point spread function (PSF) of the scanner, which we approximate with a Gaussian (G_σ). Then, we model the PVE by:

1. Estimation of the distance to the surface by Eq. (1).
2. Eq. (2) defines then the density.

First, a distance to the geometrical object is estimated for an implicit function by:

$$dist = \frac{f}{\|\nabla f\|} \tag{1}$$

f is the implicit function of the geometrical object. The PVE from the CT-Scanner with the σ parameter applied to the distance to the geometrical object. Finally, the density mean is computed by:

$$density = b + V \times G_\sigma(dist) \tag{2}$$

Then, since a convolution of a unit step with a Gaussian results in the *erfc* function, instead of G_σ, we use the *erfc* function [11]. *erfc* is defined as the complementary error function encountered in integrating the Gaussian distribution, more details in [11].

4.1 Creating an Elliptical Cross-section Model of a Vessel

An elliptical cross-section of a vessel is model using the following parameters:

- Center of the ellipse, given by (x_0, y_0)
- Radius dimensions, given by (r_x, r_y)
- Rotation angle, given by α
- A Gaussian filter with parameter σ to model the PSF from the CT-Scanner
- Mean density value V for a vessel structure
- Mean density value b for background

For a general ellipse with a rotation parameter α, its implicit function is given by:

$$f(x,y) = \frac{[(x-x_0)\cos(\alpha) - (y-y_0)\sin(\alpha)]^2}{r_x^2} + \frac{[(x-x_0)\sin(\alpha) + (y-y_0)\cos(\alpha)]^2}{r_y^2} - 1 \tag{3}$$

4.2 Creating a Cylindrical 3D Model of a Vessel

The cylindrical model is created using the following parameters:

- Center of the cylinder, given by (x_0, y_0, z_0)
- Radius dimensions of the cross-section for the cylinder, given by (r_x, r_y)
- Rotation angles around x and y axis, given by α and β
- A Gaussian filter with parameter σ to model the PSF from the CT-Scanner
- Mean density value V for a vessel structure
- Mean density value b for background

We assume a cylinder along the z-axis rotated with respect to the x axis by α, and with respect to y axis by β, centered in (x_0, y_0, z_0) (see Figure 3). A general elliptical cylinder can be modeled by the equation (4). Its general implicit function is given by:

$$\frac{[(x-x_0)\cos(\beta) + (y-y_0)\sin(\alpha)\sin(\beta) + (z-z_0)\sin(\alpha)\cos(\beta)]^2}{r_x^2} + \frac{[(y-y_0)\cos(\alpha) - (z-z_0)\sin(\alpha)]^2}{r_y^2} - 1 \tag{4}$$

Figure 4 illustrates the model data generated by a cylindrical model. We create a set of slices with elliptical cross-sections along the z-axis. This model is modulated by its parameters until it fits the data.

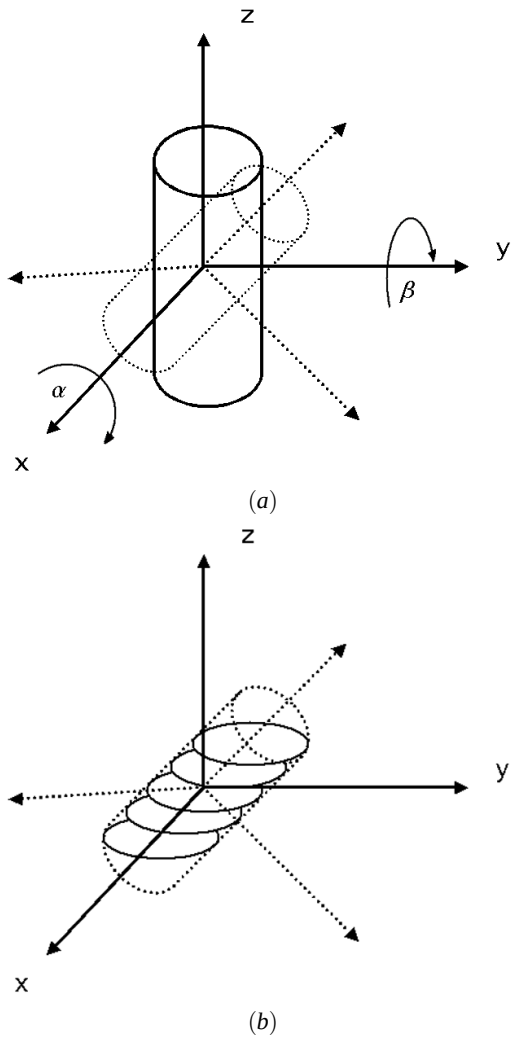

Figure 3: (a) Cylinder along the z-axis rotated with angles α and β around the x-axis and y-axis respectively. (b) Elliptical cross section along the z-axis of the rotated cylinder

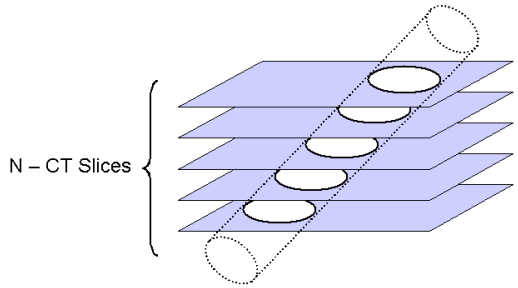

Figure 4: Illustrative example of a cylindrical model

4.3 Levenberg-Marquardt Method

The Levenberg-Marquardt method [6] is a nonlinear minimization technique. This technique can be used to fit a model to data when it depends nonlinearly on a set of M unknown parameters a_k, $k = 1,2,...,M$. The idea of the Levenberg-Marquardt algorithm is to minimize an merit function χ^2 and iteratively determine the best fitting parameters by minimization. The objective function measures the agreement between the model and the given data. In a fitting process, the parameters of the model are adjusted to achieve a minimum in the objective function. The process is repeated while χ^2 decreases or when a change in the parameters changes χ^2 by an amount $<< 1$, which is not considered statistically significant.

Assume that we are fitting N data points (x_i, y_i) $i = 1,...,N$, to a model $f(x;\mathbf{a})$ that has M adjustable parameters a_k. The model predicts a functional relationship between the measured independent (y) and dependent ($f(x;\mathbf{a})$) variables.

$$y = f(x;\mathbf{a}) \tag{5}$$

The idea is minimize the merit function χ^2 given by:

$$\chi^2 = \sum_{i=1}^{N} \left[\frac{y_i - f(x_i;\mathbf{a})}{\sigma_i} \right]^2 \tag{6}$$

where y_i is a value from an N-dimensional data, and with the same dimension $f(x_i;\mathbf{a})$ is a value from the model evaluated in $\mathbf{a}$. In our case we used 2-dimensional data for the elliptical cross-section model, and 3-dimensional data for the cylindrical model. σ_i represents a known standard deviation for each point from the data. In our case, we use $\sigma_i = 1$ by simplicity.

Given an initial estimation of parameters, $\mathbf{a}$ the Levenberg-Marquardt process consists of [8]:

(1) Compute $\chi^2(\mathbf{a})$

(2) Set an initial value for λ, say λ = 0.001. Here, λ represents a factor used in each iteration to cut down the step.

(3) Solve the linear equation $\sum_{l=1}^{M} \alpha'_{kl} \delta a_l = \beta_k$ for $\delta\mathbf{a}$ and evaluate $\chi^2(\mathbf{a}+\delta\mathbf{a})$

(4) if $\chi^2(\mathbf{a}+\delta\mathbf{a}) \geq \chi^2(\mathbf{a})$, increase λ by a factor of 10 (or any other factor) and go to (3)

(5) if $\chi^2(\mathbf{a}+\delta\mathbf{a}) < \chi^2(\mathbf{a})$, decrease λ by the same factor as in (4), update the trial solution $\mathbf{a}$ by $\mathbf{a}+\delta\mathbf{a}$ and go back to (3)

where

$$\begin{aligned} \alpha'_{jj} &\equiv \alpha_{jj}(1+\lambda) \\ \alpha'_{jk} &\equiv \alpha_{jk} \qquad (j \neq k) \end{aligned} \tag{7}$$

and $\delta\mathbf{a}$ represent the steepest descendent formula, and for each parameter a_l, δa_l is given by:

$$\delta a_l = \frac{1}{\lambda \alpha_{ll}} \beta_l \tag{8}$$

and

$$\alpha_{kl} = \sum_{i=1}^{N} \frac{1}{\sigma_i^2} \left[\frac{\partial y(x_i;\mathbf{a})}{\partial a_i} \frac{\partial y(x_k;\mathbf{a})}{\partial a_l} \right] \tag{9}$$

5 Results

As first result, we apply both model fitting to a synthetic data set. This should illustrate that both methods produce quite similar results concerning the curvature (see Figure 5).

The synthetic data set consists of 3D data of 256x256x768 voxels with size 0.5^3mm. The diameter varies along the z-axis from about 0.7 to about 23 voxels, simulating the size-range of arterial vessels imaged with CT. The density is defined between 1130 and 1350 and the background density between 1080 and 1100 (which corresponds to CT attenuation values of 130 to 350, and 80-100 Hounsfield Units, respectively). The curvature of the vessel is simulated by a helix with an angle of 32.14 and radius of 76.8 voxels.

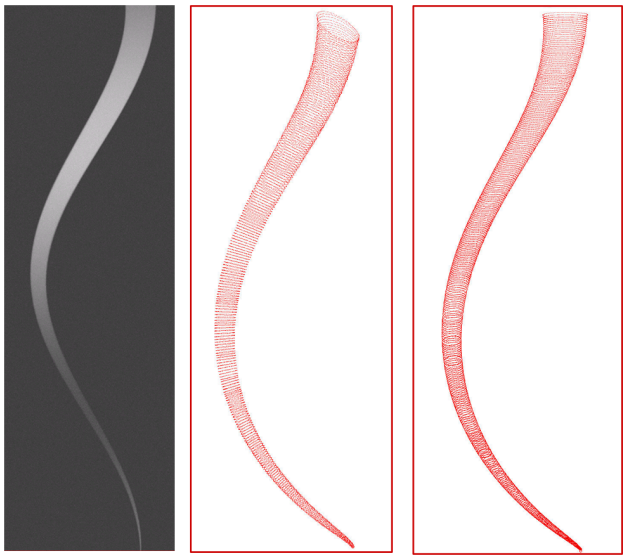

Figure 5: Result on synthetic data. Left, MIP image of the synthetic data, followed by elliptical cross-section model fitted along the vessel path, and finally a parameterized vessel by cylindrical model fitting

We apply the cylindrical model fitting to a real patient dataset in a region of interest where manual segmentation by experts is required (see Figure 2). Figures 6 and 7 show the result of fitting an initial model to a set of ten slices of volumetric data, starting from an initial seed point. In the Figures, the first and last columns of images correspond to the first and the last slice of a sub-volumetric region defined by a set of 10 slices (as an example). The center column of images correspond to the slice in the middle of the dataset. The upper row of images corresponds to a partially occluded vessel. The second row of images corresponds to the fitted model. Finally, the third row is a super position of the cylinder enclosing the vessel. Here, we can see that there is not a clear distinction between the vessel boundary and soft tissue or vessel background. It looks like a bifurcation, but it is not. This is certainly a difficult case where any other preprocessing step using derivative estimation, gradient information or thresholds are likely to fail. However the cylindrical

vessel model fits quite well to the sub-volumetric data of the vessel. Figure 7 shows the result on a calcified vessel. This is also a difficult case to segment. From the medical point of view it is quite important to extract the entire vessel dimensions, rather than the lumen only, because it allows an estimation of the relative degree of a stenosis. In both cases (from Figures 6 and 7) the density of the fitted model corresponds to the mean density for the data. This would help to combine this technique with an adaptive process to correct for inter- and within-individual variation of the degree of vascular opacification, and to distinguish vessel from other structures, such as bone.

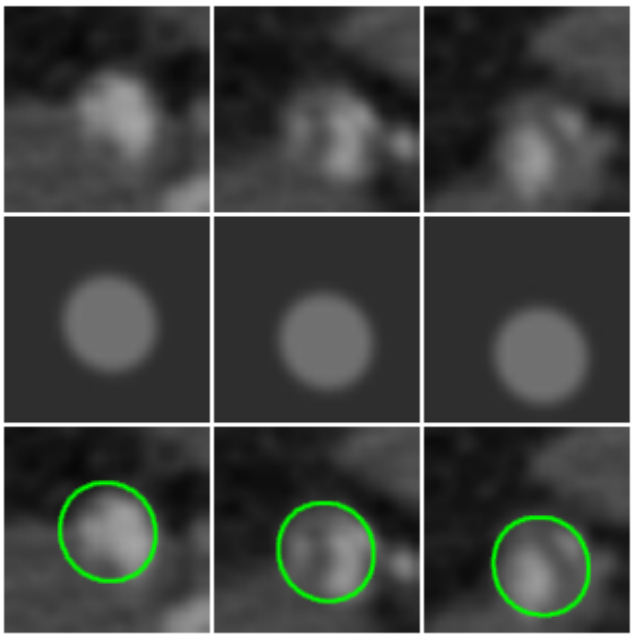

Figure 6: Result of fitting on a vessel with a partial occlusion

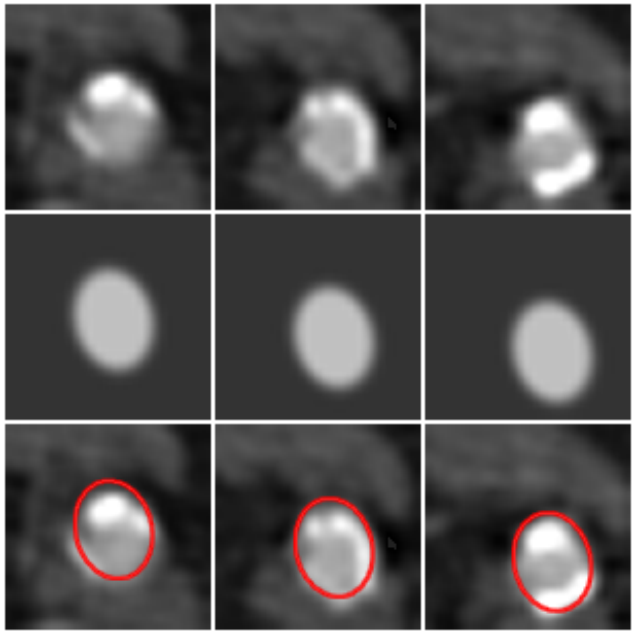

Figure 7: Result of fitting on a calcified vessel

Finally, we present a comparison of the cylindric model with a clinical application. It is based on the ray casting technique (RCT) developed by Kanitsar et al. [2] and evaluated in [5] as a good approximation of the vessel centerline. Figure 8 presents the center path generated by the RCT technique (see Figure 8(a)) and the cylindrical model fitting (see Figure 8 (b)). Here, we can see how the centerline generated by the RCT is not actually in the vessel-center. The centerline extracted from the cylindrical model fitting looks more centered (see zoomed circular area, showed in Figures 9(a) and (b)).

Figures 9 (a) and (b), are particularly relevant because they show one of the limitations of the CPR [2] visualization technique, which is its dependence on an accurate centerline estimation. An off-axis reformatting surface for the CPRs causes artificial vessel narrowing or 'pseudo-stenosis' in the resulting image (see zoomed circular window in Figure 9). Figures 9 also allow us to compare visually that the cylindrical model fitting gives a better center approximation and avoids the generation of artificial stenosis in the CPR images. The vessel segmented in Figure 10 is characterized by a complex pattern of densities within the diffusely diseased left femoral artery. There are pockets of residual lumen (light grey), irregular areas of non-calcified plaque (dark grey), and areas of calcified atherosclerotic plaque (white). Even though, the centerlines and CPR images from the cylindrical model fitting are more accurate than the RCT based results, and compare favorably to those based on expert user interactions.

6 Conclusion

This work presents a strategy to parameterize a vascular structure from a vessel model by a non-linear fitting process. The Levenberg-Marquardt method is used as a non-linear minimization process, which allows to extract optimal parameters from a model that best fits the data.

In this paper, we present a segmentation solution in cases where classical segmentation methods fail. Diseased vessels show a wide variability of density values, which makes it difficult to detect the vessel boundary. A cylindrical model fitting requires neither a preprocessing step nor any operator estimation, such as, gradient, derivative, etc.

The cylindrical model fitting can be considered as initial step to implement an automatic segmentation of vascular structures. Future work should address the following issues: performance, handling of vessel bifurcations, and inclusion of further anatomical knowledge.

7 Acknowledgement

This work was supported by the Austrian Science Fund (FWF) grant No. P15217. (AngioVis).

References

[1] K. Bühler, P. Felkel, and A. La Cruz. Geometric Methods for Vessel Visualization and Quantification - A Survey. In *Geometric Modelling for Scientific Visualization*, pages 399–420. G. Brunnet, B. Hamann and H. Müller and L. Linsen (eds.). Kluwer Academic Publishers, 2003.

[2] A. Kanitsar, R. Wegenkittl, P. Felkel, D. Fleischmann, D. Sandner, and E. Gröller. Computed Tomography Angiography: A Case Study of Peripheral Vessel Investigation. In *IEEE Visualization 2001*, pages 477–480, October 2001.

[3] C. Kirbas and F.K.H Quek. A Review of Vessel Extraction Techniques and Algorithms. Technical Report, VisLab Wright State University, Dayton, Ohio, Nov 2000.

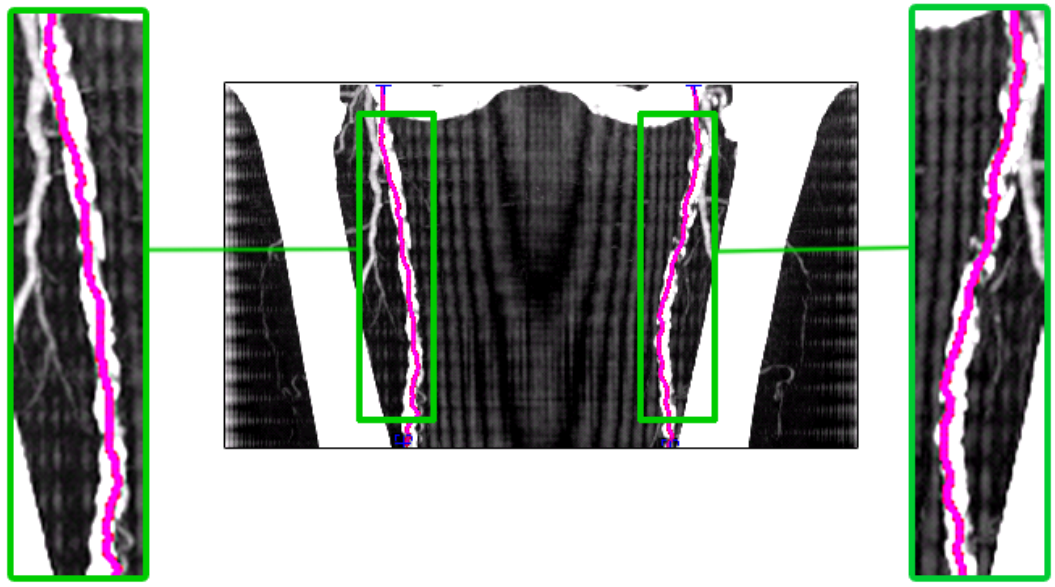

(*a*)

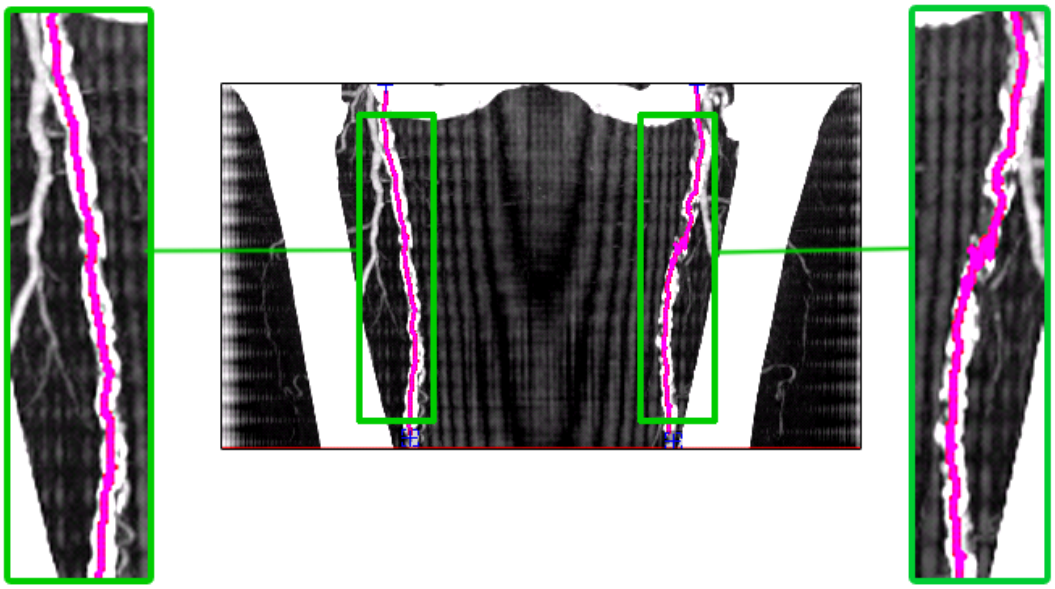

(*b*)

Figure 8: MIP images with superimposed centerline generated by (a) the RCT technique and (b) the cylindrical model fitting. Note, that patient images are shown as if viewed from the front of the patient. The right femoral artery is thus on the left side of the image.

[4] K. Krissian, G. Malandain, and N. Ayache. Model Based Multiscale Detection and Reconstruction of 3D Vessels. Technical Report 3342, INRIA, Jun 1998.

[5] A. La Cruz. Accuracy Evaluation of Different Centerline Approximations of Blood Vessels. In *The Proccedings of Symposium on Visualization VisSym 2004 (To appear)*. IEEE, 2004.

[6] D. W. Marquardt. An Algorithm for Least-Squares Estimation of Nonlinear Parameters. *Journal of the Society for Industrial and Applied Mathematics*, 11:431–441, 1963.

[7] T. McInerney and D. Terzopoulos. Topology Adaptive Deformable Surfaces for Medical Image Volume Segmentation. *IEEE Transactions on Medical Imaging*, 18(10):840–850, 1999.

[8] W. Press and W. Vettering B. Flannery, S. Teukolsky. *Numerical Receipes in C*. Cambridge University press, Cambridge, 1992.

[9] M. Straka, A. La Cruz, A. Köchl, L. I. Dimitrov, M. Šrámek, D. Fleischmann, and E. Gröller. Bone Segmentation in CT-Angiography Data Using a Probabilistic Atlas. In *Vision Modeling and Visualization*, pages 505–512, Nov 2003.

[10] M. Šrámek and A. Kaufman. Object Voxelization by Filtering. In *The Proccedings of IEEE Symposium on Volume Visualization*, pages 111–118. North Carolina, 1998.

[11] E. Weisstein. *CRC Concise Encyclopedia of Mathematics*. Boca Raton, FL: CRC Press, 1998.

[12] O. Wink, W.J. Niessen, and M.A. Viergever. Fast Delineation and

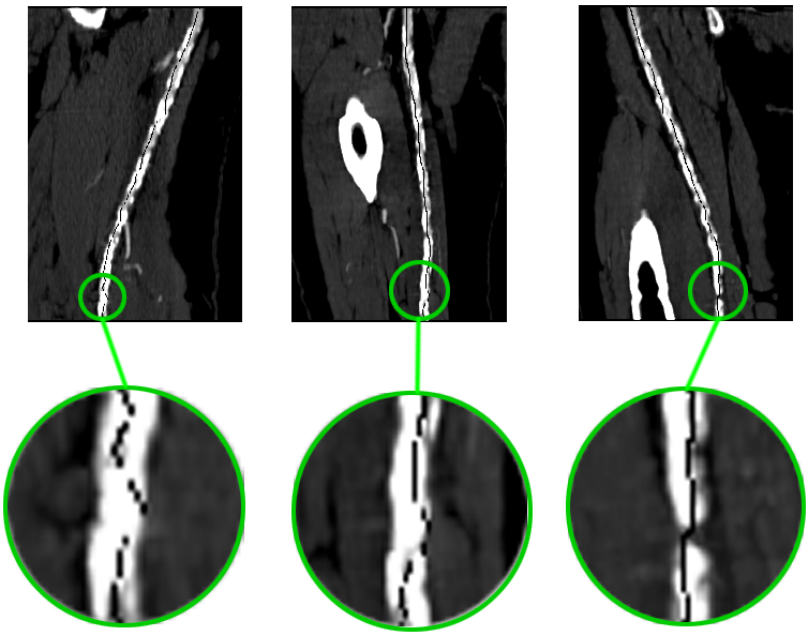

(*a*)

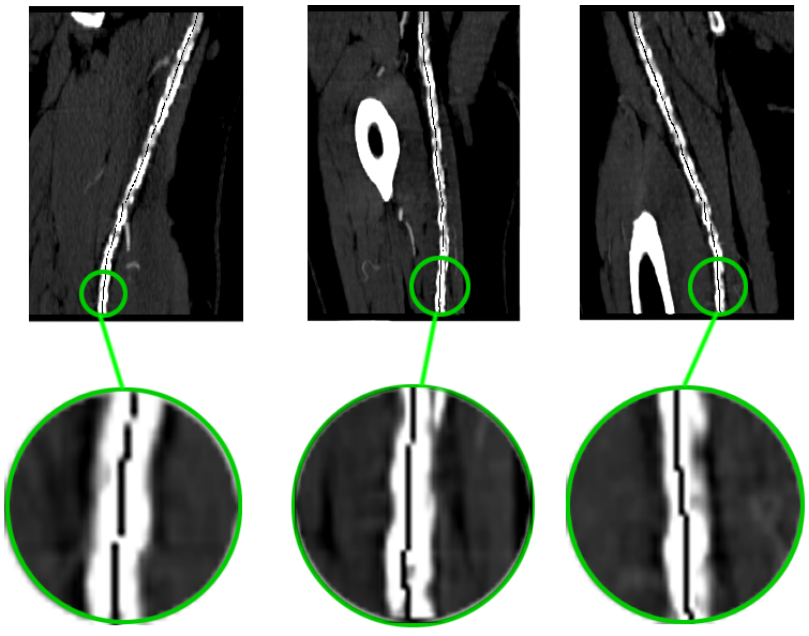

(*b*)

Figure 9: CPR images of the right femoral artery from the same dataset as figure 8, viewed from three different angles (- 90dgr [as if viewed from the right side of the patient], 0 dgr [viewed from the front of the patient], and 45 dgr [as if viewed from an oblique left standpoint relative to the patient]), with superimposed center-paths. Images in panel (a) were created from the RTC-based centerline approximation, Images in panel (b) were created with cylindrical model fitting. Zoomed images illustrate the improved approximation of the central path with the cylindrical model fitting technique. Note the artifactual high-grade stenosis in the 45dgr view in (a), which is caused by the eccentric course of the centerline path.

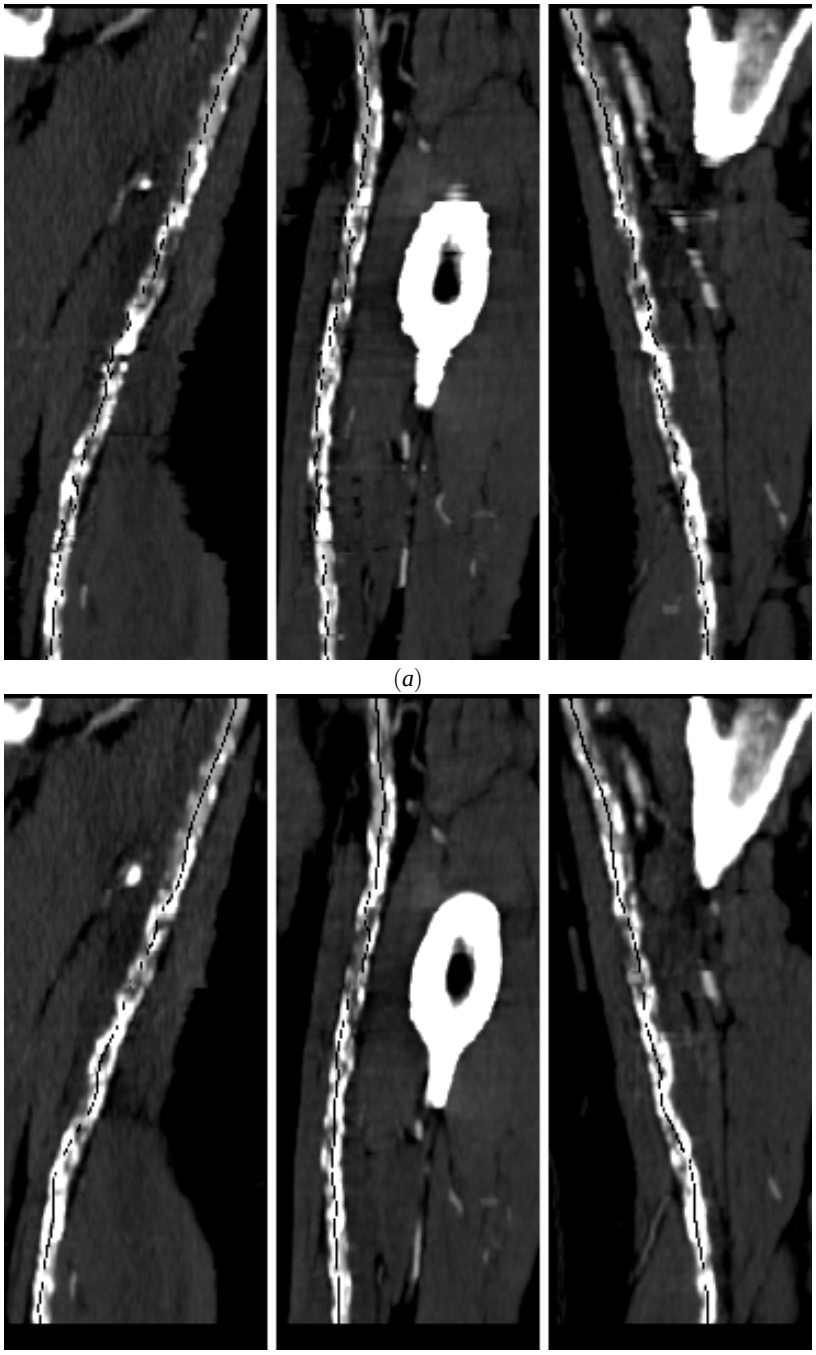

(*a*)

(*b*)

Figure 10: CPR images of the left femoral artery from the same dataset as figure 8, viewed from three different angles (- 90dgr [as if viewed from the right side of the patient], 0 dgr [viewed from the front of the patient], and 45 dgr [as if viewed from an oblique left standpoint relative to the patient]), with superimposed center-paths. Images in panel (a) were created from the RTC-based centerline approximation, Images in panel (b) were created with cylindrical model fitting. Note the improved course of the centerline in (b) in this example of complex attenuation of the diseased blood vessel, caused by residual lumen, hypodense (non-calcified) plaque, and hyperdens calcified plaque.

Visualization in 3-D Angiographic Images. *IEEE Transactions on Medical Imaging*, 19(4):337–346, 2000.